Biochimica et Biophysica Acta 1830 (2013) 3570–3577

Contents lists available at SciVerse ScienceDirect

Biochimica et Biophysica Acta

journal homepage: www.elsevier.com/locate/bbagen

The allosteric modulation of thyroxine-binding globulin affinity is entropy driven

Ariel A. Petruk [a,*], María S. Labanda [b], Rosa M.S. Álvarez [a,b], Marcelo A. Marti [c,**]

[a] Instituto Superior de Investigaciones Biológicas (INSIBIO-CONICET), Chacabuco 461, S. M. de Tucumán, Tucumán, T4000ILI, Argentina
[b] Instituto de Química Física, Faculad de Bioquímica, Química y Farmacia, Universidad Nacional de Tucumán, San Lorenzo 456, S. M. de Tucumán, Tucumán, T4000CAN, Argentina
[c] Departamento de Química Biológica e INQUIMAE-CONICET, Facultad de Ciencias Exactas and Naturales, Universidad de Buenos Aires, Ciudad Universitaria, Pabellón 2, Buenos Aires, C1428EHA, Argentina

ARTICLE INFO

Article history:
Received 13 July 2012
Received in revised form 20 February 2013
Accepted 22 February 2013
Available online 1 March 2013

Keywords:
Serpin family
Thyroxine-binding globulin
Allostery
Conformational entropy
Generalized Born surface analysis
Molecular dynamics

ABSTRACT

Background: Thyroxine-binding globulin (TBG) is a non-inhibitory member of the serpin family of proteins whose main structural element is the reactive center loop (RCL), that, upon cleavage by proteases, is inserted into the protein core adopting a β-strand conformation (stressed to relaxed transition, S-to-R). After S-to-R transition thyroxine (T4) affinity decreases. However, crystallographic studies in the presence or absence of the hormone in different states are unable to show significant differences in the structure and interactions of the binding site. Experimental results also suggest the existence of several S states (differing in the number of inserted RCL residues), associated with a differential affinity.
Methods: To shed light into the molecular basis that regulates T4 affinity according to the degree of RCL insertion in TBG, we performed extended molecular dynamics simulations combined with several thermodynamic analysis of the T4 binding to TBG in three different S states, and in the R state.
Results: Our results show that, despite T4 binding in the protein by similar interactions in all states, a good correlation between the degree of RCL insertion and the binding affinity, driven by a change in TBG conformational entropy, was observed.
Conclusion: TBG allosteric regulation is entropy driven. The presence of multiple S states may allow more efficient T4 release due to protease activity.
General significance: The presented results are clear examples of how computer simulation methods can reveal the thermodynamic basis of allosteric effects, and provide a general framework for understanding serpin allosteric affinity regulation.

1. Introduction

It is well known that thyroid hormones exert profound effects on the metabolism, growth and development of vertebrates. About 97.5% of the circulating thyroid hormones consist of thyroxine (T4), and 75% of this is bound to the thyroxine-binding globulin (TBG) [1]. TBG is a medium sized globular protein, structurally related to the archetypal serine protease inhibitor (serpin), the α1-antitrypsin (αAT). A phylogenetic study of the superfamily, divided the eukaryotic serpins into 16 'clades' (termed A to P). Both TBG and αAT are clade A members [2]. However, unlike most serpins, TBG is not known as a protease inhibitor but appears to be an active hormone carrier and a substrate of specific proteases. This suggests that TBG has the capacity to control the delivery of the thyroxine in sites of inflammation. Structurally, serpins constitute a family with a single core domain composed by three β-sheets (termed sA-sC) and 8–9 α-helices (termed hA–hI) [3]. One of the most important structural elements of these proteins is the reactive center loop (RCL) that connects the β-sheet A to the β-sheet C, and which is completely exposed to the solvent (Fig. S1B). Target proteases recognize and cleave the RCL. Upon cleavage, the fragment composed by the RCL is inserted into the β-sheet A and forms a novel β-strand called the s4A strand (Fig. S1C), which results in a conformational change known as "stressed to relaxed" (S-to-R) transition [2]. In TBG this S-to-R transition is associated with an increase in thermostability and with a decrease in ligand binding affinity [4–6]. Based on these observations it has been proposed that the serpin structure has been adapted by TBG to control the hormone release at this site of action, after the RCL is proteolytically cleaved.

In order to understand how the decrease in affinity is induced by the S-to-R transition, several structural studies of TBG and other serpins in different states have been performed during the past decade. For example, the TBG structurally related native rat corticosteroid-binding globulin (CBG) bound to cortisol was crystallized (PDB ID: 2v95) [7]; this showed the typical S state conformation of native serpin (i.e. with the

* Corresponding author. Tel.: +54 3814213226.
** Corresponding author. Tel.: +54 1145763380.
E-mail addresses: apetruk@fbqf.unt.edu.ar (A.A. Petruk), marcelo@qi.fcen.uba.ar (M.A. Marti).

0304-4165/$ – see front matter © 2013 Elsevier B.V. All rights reserved.
http://dx.doi.org/10.1016/j.bbagen.2013.02.023

RCL completely exposed, Fig. S1A). Interestingly, the X-ray structure of native TBG with thyroxine bound (PDB ID: 2ceo [8], Fig. S1B) shows the RCL residue Gly341 already inserted into the β-sheet A [8]. The conformations adopted by the RCL in both mentioned proteins correspond to the S state [7,9]. In this work, we will refer to them as S0 and S1 in order to differentiate between the completely exposed RCL, from that with one residue (Gly342) incorporated into the β-sheet A. The crystal structure of the TBG wild type with the RCL cleaved (R state) is not available. The structure with the fully incorporated RCL fragment into the β-sheet A (Fig. S1C), which corresponds to the R state, is then provided by the crystal structure of a cleaved, T4 bound, TBG Pittsburg chimera (i.e. with the sequence of the RCL corresponding to that of the αAT, αAT–T4–cTBG, PDB ID: 2riw [10]). Comparison of the mentioned structures led to the surprising observation that the residues composing the thyroxine or corticosteroid binding sites show the same structures and interactions with the hormones, whether the proteins were in the S or R states [10]. These results thus prevent any structural rationalization related to the change in affinity. Besides the mentioned structural studies, in-vitro ligand binding studies performed with several mutants and chimeras TBG and CBG, strongly suggested that, in addition to the fully exposed RCL (S state) and the completely inserted RCL (R state), other intermediate S states, with different degrees of RCL insertion, are also possible (Fig. 1). These results also showed that the intermediates S states differ in their ligand binding affinity [7,10–13]. The structural origin of the difference in affinity, however, remains unknown.

Usually, allosteric modulation of a ligand affinity, as observed for TBG in the S-to-R transition, is associated with the presence of key structural differences in the binding site. These differences result in specific changes of the protein–ligand interactions, which in turn reduce or increase the ligand binding enthalpy and, subsequently, the ligand binding free energy. In this sense, allosteric modulation is said to be enthalpy-driven. However, there are reported cases exhibiting allosteric regulation even though no significant structural changes associated with the ligand binding or allosteric process are observed [14]. In those cases, the enthalpy changes cannot explain the allosteric behavior, and the role of entropy changes must be considered. Entropy undoubtedly plays a key role in the ligand binding process, and has a great potential as an affinity modulation mechanism. Due to its intrinsic dynamic nature, experimental studies of entropic effects are difficult, and just recently NMR techniques, which explicitly reveal protein dynamics, have allowed tackling this subject systematically. On the other hand, computer simulation techniques such as molecular dynamics (MD) have great potential to analyze the role played by dynamical and entropic effects on molecular processes and particularly, on ligand binding to proteins. See for example our recent review on the topic [15].

Taking advantage of this mentioned potential of computer simulation techniques, and in order to provide a better picture of how the different S states and the S-to-R transition in TBG modulate the T4 affinity, we present here results of extended MD simulations of TBG in several representative conformational states, with and without the hormone. Specifically, three different conformations of the uncleaved RCL were simulated, which were characterized as the S0, S1 and S3 stressed states of the protein, and according to the loop, were completely exposed, with one, and with three residues inserted into the β-sheet A, respectively. The relaxed R state of the TBG was also simulated (Fig. 1). Similar to previous crystallographic data, our results show no significant structural differences in the binding site of TBG in all the studied states, regardless of whether the hormone was present or not. However, distinctions in the binding affinity between the different S states and the R states were found to be dependent on the protein conformational entropy change, thus providing another example of an entropy mediated allosteric effect.

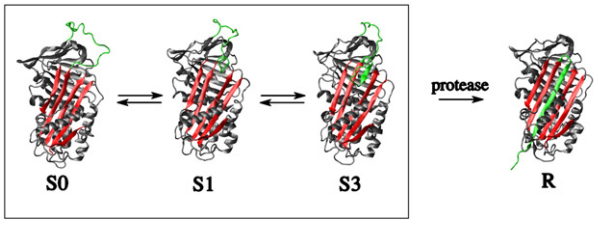

Fig. 1. TBG posed states (RCL in green and s4A in red): three different simulated SX states are shown, where X = 0, 1 and 3 corresponds to the number of the RCL residues inserted as strand s4A. The R state shows the fully incorporated RCL. Structures were built as described in Methods and schematically presented in the Supporting Information (Fig. S2).

2. Methods

2.1. Classical molecular dynamics simulation and parameters

In order to study the dynamical properties of TBG in the possible S and R states and their relations with the ligand binding affinity, we performed MD simulations of both, the free protein and the protein complexed with T4, in three different conformations corresponding to the S state and one conformation corresponding to the R state (as shown in Fig. 1). The procedure to generate the initial structures of the MD is depicted in Fig. S2. The starting coordinates for the S0 and S1 states of TBG, with and without the hormone, were extracted from the crystal structure of wild type thyroxine bound human TBG (PDB ID: 2ceo [8]). The T4–TBG-S1 system, which corresponds to the native uncleaved T4–TBG complex with Gly341 inserted into the β-sheet A, was built from the crystal structure directly. The T4–TBG-S0 system was built by removing the original RCL and adding a new RCL fragment, totally exposed to the solvent. The T4–TBG-S3 system containing the uncleaved RCL with the Gly340, Thr341 and Glu342 residues inserted into the β-sheet A, was built from T4–TBG (PDB ID: 2ceo [8]) and from αAT–T4–cTBG (PDB ID: 2riw [10]) with the MODELER v9 program [16]. The αAT–T4–cTBG crystal structure was also used to build the T4–TBG-R system, that contains the RCL cleaved and completely inserted as the s4A strand, but in this case the chimeric amino acids were replaced by those of the wild type structure. Since all the crystal structures showed partially unsolved RCL, the MODELER v9 program [16] was used to perform the structural modification and to add the missing amino acids in the generated structures. Removals of thyroxine from each system yielded the hormone free TBG-S0, TBG-S1, TBG-S3 and TBG-R structures, respectively.

All the starting structures were immersed in a preequilibrated octahedral box of TIP3P water molecules. The standard protonation state at physiological pH was assigned to ionizable residues. Special attention was paid to the protonation of histidines, which were assigned on the basis of the hydrogen-bond pattern with neighbor residues. Each final system contained ~14,000 water molecules. All simulations were performed at 300 K and pressure of 1 bar using the Berendsen thermostat and barostat [17]. Periodic boundary conditions and Ewald sums (grid spacing of 1 Å) were used to treat the long range electrostatic interactions. The SHAKE algorithm was used to keep bonds involving hydrogen atoms at their equilibrium lengths [18]. A 2 fs time step for the integration of Newton's equations was used. The Amber99SB force field [19] was used for all residues, while for thyroxine the general AMBER force field [20] was used. The point charges for thyroxine were taken from our previous work [21]. All simulations were performed with the PMEMD module of the AMBER11 package [22].

The equilibration process consisted of an energy minimization of the initial structures, followed by a slow heating up to 300 K performed in 3 steps of 60 ps at 100, 200 and 300 K, respectively. Production simulations consisted in 200 ns long MD trajectories for each system (this group of simulations is called “set 1”). The backbone atoms of the three residues constituting the partial s4A strand in

the S3 states were slightly restrained during the first 10 ns of the simulated time. A second independent 100 ns long trajectory was obtained for each system. These independent simulations were performed by assigning new random velocities to randomly selected snapshots extracted from the 90–100 ns time segment of the initial simulation (set 1), and no restraint was applied. They constitute the "set 2" of simulations. The total simulated time was 2.4 μs.

2.2. Analysis of the MD trajectories and calculation of thermodynamic properties

The equilibrated 100 ns (for the two sets of simulations) of the trajectory of each system, was analyzed with the PTRAJ [22] and VMD [23] programs. First, RMSd and RMSf plots were done with the widely known equations. To estimate the statistical error in the RMSf vs residue plots, we performed block average analysis dividing the 100 ns equilibrated simulation time into 2 blocks of 50 ns and into 4 blocks of 25 ns, and combining the blocks from the two simulation sets. Reported error values correspond to the maximum standard deviation of the resulting block combination. Regarding the thermodynamic analysis, end-point binding single trajectory free energy decomposition analysis was done using the Molecular Mechanics Generalized Born Surface Area (MM-GBSA) [24,25] method as implemented in the AMBER package of programs. The method applied to the protein–ligand complex in the single trajectory approach computes the different components, like Van der Waals and electrostatic interaction energies (ΔE_{VdW} and ΔE_{elec}, respectively), and difference in solvation free energy (ΔG^{solv}), that contribute to the binding free energy (using directly the force field parameters). The difference in solvation free energy is computed using the GBSA implicit solvation approximation which includes both cavitation and electrostatic contributions [24]. Previous works from our group have shown that although the method may overestimate the total binding free energy, it can be used with confidence [26,27] to analyze differences in the binding free energy between different ligands to the same protein, or for the same ligand in different proteins or protein states [15,28], as in the present case.

To determine the configurational entropy contributions of both, the ligand and, more importantly, the protein we used the approximation developed by Andricioaei–Karplus [29]. In this method, the entropy determination is based on a quasi-harmonic approximation using the protein Essential Modes (EM). The EM are computed by diagonalization of the Cartesian atomic position mass-weighted covariance matrix, using only the backbone atoms. The diagonalization yields a collection of eigenvectors representing the collective protein motions, and a set of eigenvalues that measures the corresponding mode amplitudes, which directly relate to the mode frequencies, according to:

$$\omega_i = \sqrt{k_B T/\lambda_i} \tag{1}$$

where ω_i is the EM frequency and λ_i the EM eigenvalue. The entropy in the Andricioaei–Karplus method is then computed by Eq. (2).

$$S_{Andr} = k\sum_{i}^{3N-6}\left[\frac{\hbar\omega_i/k_BT}{e^{\hbar\omega_i/k_BT}-1} - \ln\left(1-e^{-\hbar\omega_i/k_BT}\right)\right] \tag{2}$$

where, the sum is performed over all the EM with frequency ω_i, and where $\hbar$ and k_B are the Planck and Boltzmann constants respectively. T is the system temperature.

The EM and the estimated entropy, are strongly dependent on the conformational space sampled. Increased sampling results in larger modes and more entropy. Since conformational space sampling is largely dependent on the simulation time scale, the calculated entropy also depends on the length of the trajectory used for the determination of the EM. Therefore, in order to obtain a value which is independent of the trajectory length (i.e. as well converged as possible), we computed the entropy values for each system/state for different increasing time intervals (using 500, 1000 or 1500 snapshots). The corresponding reported infinite time (or time independent) entropy values (S_∞), were finally obtained by linearly fitting the extensively tested Eq. (3):

$$S(t) = S_\infty + \alpha t^{-1} \tag{3}$$

In this equation S_∞ corresponds to the limit entropy value at infinite simulation time, α is a numerical constant obtained from the fitted procedure, t is the time interval, or length of the trajectory used to determine the EM and thus, the time dependent entropy values, $S(t^{-1})$. These values were computed solely for the equilibrated segment of the whole simulation time (usually the last 75 ns) [27,30–33].

Comparison among different pairs of EM was performed using the similarity index (SI), which is the dot product between two selected eigenvectors from the EM analysis:

$$SI_{AiBj} = \nu_{Ai}\cdot\nu_{Bj} \tag{4}$$

were Ai corresponds to EM number "i" of MD simulation "A". Values close to 1 mean that both modes are almost identical, whereas values close to zero indicate completely orthogonal or different modes [34].

3. Results

3.1. Stability and convergence of TBG MD simulations

We first analyzed the proper relaxation of each system until an equilibrated ensemble was obtained. To this purpose, we computed RMSd vs time plots for each system using the initial structure as reference (Fig. S3). In general, the RMSd shows small values, averaged between 1.30 and 2.45 Å. The higher RMSd values were for the S0 and S1 states and the lower for the S3 and R states (Table S1). This indicates that all systems were stable at the simulated temperature, showing only local native state fluctuations. Moreover, as expected from crystallographic data, the RCL in all the S systems did not adopt any particular structure or configuration, but fluctuated randomly during the whole MD.

In order to analyze the TBG flexibility in the different states and its relation to T4 binding we computed the RMSf for each residue combining both simulation sets for each system. The results are shown in Supplementary Information Fig. S4. Strikingly, in general the RMSf patterns are very similar for all cases, and no systematic change is observed upon T4 binding. The RCL is, by far, the most flexible region, especially in the S0 and S1 states. Interestingly, its mobility is already significantly reduced in the S3 state and absent in the R state. Thus, apart from the RCL, there seems not to be a significant change in the flexibility of the different protein regions in the bound/unbound states in any of the studied systems.

3.2. Structure and dynamics of the hormone binding site

The interactions between thyroxine and TBG were first reported by Zhou et al. after solving the crystal structure of T4–TBG in the S state [8]. Recently, Qi et al. published similar results for the αAT–T4–cTBG chimeric structure [10]. In Fig. 2A, a snapshot extracted from our T4–TBG-S0 MD simulation describes the binding site structure. Thyroxine appears bound to the protein mainly by VdW and two key hydrogen bond interactions involving the Asn273 and Arg378 residues. We characterized this interaction by measuring the distance between the mass center of the heavy atoms of the

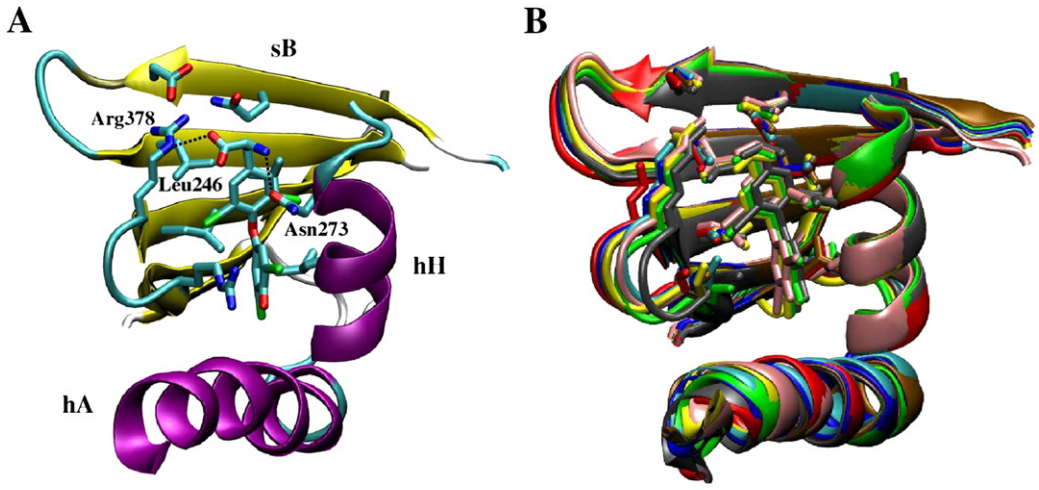

Fig. 2. (A) Snapshot of a representative T4–TBG-S0 structure showing the thyroxine bound to the hormone binding site; hA, hH and sB secondary structure elements are shown. (B) Average structures over both simulation sets of the thyroxine binding pocket of the eight studied systems, T4–TBG-S0 (gray), TBG-S0 (red), T4–TBG-S1 (green), TBG-S1 (blue), T4–TBG-S3 (yellow), TBG-S3 (ochre), T4–cTBG-R (pink) and cTBG-R (cyan).

non-phenolic thyroxine ring and that of the C atoms of the Leu246-$CH(CH_3)_2$ group. This distance remained fairly constant throughout the simulated time in all systems (S0, S1, S3 and R) with an average value of 4.5 ± 0.3 (standard deviation) Å. The NH_3^+ group of T4 was hydrogen-bonded to the carboxyl Oδ atom of the Asn273 side chain, evidenced by a mean distance of 2.9 ± 0.2 Å between the involved heavy atoms; while the $-CO_2^-$ group of the hormone acted as hydrogen bond acceptor from the Nε group of Arg378, with an average O···N distances of 3.1 ± 0.5 Å. These results show good agreement with the reported crystal structures of T4–TBG and αAT–T4–cTBG [8,10].

We also compared the average structures of the T4 binding site obtained for each simulated TBG protein, with and without the respective bound hormone. In order to compare by visual inspection the effects produced by the RCL insertion and/or T4 binding on the binding site architecture, the average structure of each simulated system is superimposed in Fig. 2B. In agreement with the reported crystallographic analysis of the TBG protein in the different evaluated states [8,10], the MD simulations show that the binding site structures remained almost unchanged, regardless of the degree of the RCL insertion or the presence of T4 in its corresponding binding site.

3.3. Thermodynamic characterization of the hormone binding affinity

Due to the fact that we do not observe structural differences which could be related with the modulated T4 affinity in the different TBG states, we performed a detailed calculation of the thermodynamic quantities that contribute to the hormone binding free energy (ΔG_B) as described by the Eq. (5),

$$\Delta G_B = \Delta E^{\text{int.}} + \Delta G^{solv} - T\Delta S_{\infty}^{TBG} - T\Delta S_{\infty}^{T4}. \quad (5)$$

The protein–hormone interaction energy in each complex (ΔE^{int}) is computed directly from the corresponding complex simulation using the MM-GBSA method [24,25] and includes both the VdW and the electrostatic interactions ($\Delta E_{VdW} + \Delta E_{elec}$). The ΔG^{solv} term corresponds to the change in solvation free energy due to the complex formation. ΔG^{solv} includes both, the enthalpic and entropic terms related to the solvent reorganization, and is computed using the implicit solvation GBSA method. The single trajectory approach used here, has been shown to improve the accuracy of the results [15,26]. Changes in the configurational (or conformational) entropies of the hormone and the protein upon the complex formation ($T\Delta S_{\infty}^{T4}$ and $T\Delta S_{\infty}^{TBG}$, respectively) were computed using the quasi-harmonic approximation described in Methods [29]. All the computed thermodynamic parameters were averaged combining the two previously described simulation sets. Fig. 3 shows TS^{TBG} calculated with Eq. (2) for the last 75 ns of each system, and the resulting linear fit to Eq. (3), used to obtain the final entropy values at infinite simulation time. The entropy values were computed considering 500 snapshots (similar $T\Delta S^{TBG}$ trend is obtained considering 1000 or 1500 frames as shown in Table S2). The figure shows that, although the fit is not perfect, the trend and sign of the resulting $T\Delta S^{TBG}$ are clearly evidenced, and well converged for each system.

The purpose of this analysis was to elucidate which of these terms is (or are) responsible for the decrease in the binding affinity after the partial or total RCL insertion. Table 1 lists the values obtained for the corresponding thermodynamic parameters associated to T4 binding for all the studied TBG states. It should be noted that although this strategy may overestimate the ΔG_B it can be used with confidence for comparative purpose in the present case. VdW interaction energies between thyroxine and TBG were almost the same whether the RCL was in any of the S states or in the R state. The most significant difference in the electrostatic contributions was of −7 kcal/mol. Interestingly, the ΔG^{solv} values showed differences of comparable magnitude to it, although of opposite sign, so that they almost compensate each other (the sum $\Delta E_{elec} + \Delta G^{solv}$ is always close to 3–6 kcal/mol). This compensation of ΔE_{elec} and ΔG^{solv} is not unexpected, since when comparing binding for the same ligand as in the present case the major contribution to ΔG^{solv} is electrostatic (cavitation energy remains almost constant). The hormone entropy change ($T\Delta S_{\infty}^{T4}$) showed that T4 experiences a similar loss of entropy upon binding for all the studied RCL conformations. Thus, the partial contribution to the binding free energy coming from these parameters was practically the same for all the RCL states evaluated. Considering that T4–TBG interactions were similar in all studied states, these thermodynamic results were not unexpected, and corroborated previous observations that had indicated that the change in affinity for T4 has no appreciable structural (or enthalpic) origin.

Contrary to that observed for the above described contributions to the binding free energy, the change in the protein conformation entropy upon T4 binding ($T\Delta S_{\infty}^{TBG}$) showed a clear and significant difference between each of the studied states (Table 1). While for the S0 and the S1 states the conformational entropy contribution to the binding free energy was positive, indicative of an increased affinity, in the S3 and R states the conformational entropy change upon binding was negative, then the G_B increased and the TBG affinity for T4 lowered. Thus, even if the actual values of the ΔG^{solv} are approximate, the change in the sign is compelling evidence that entropy plays key

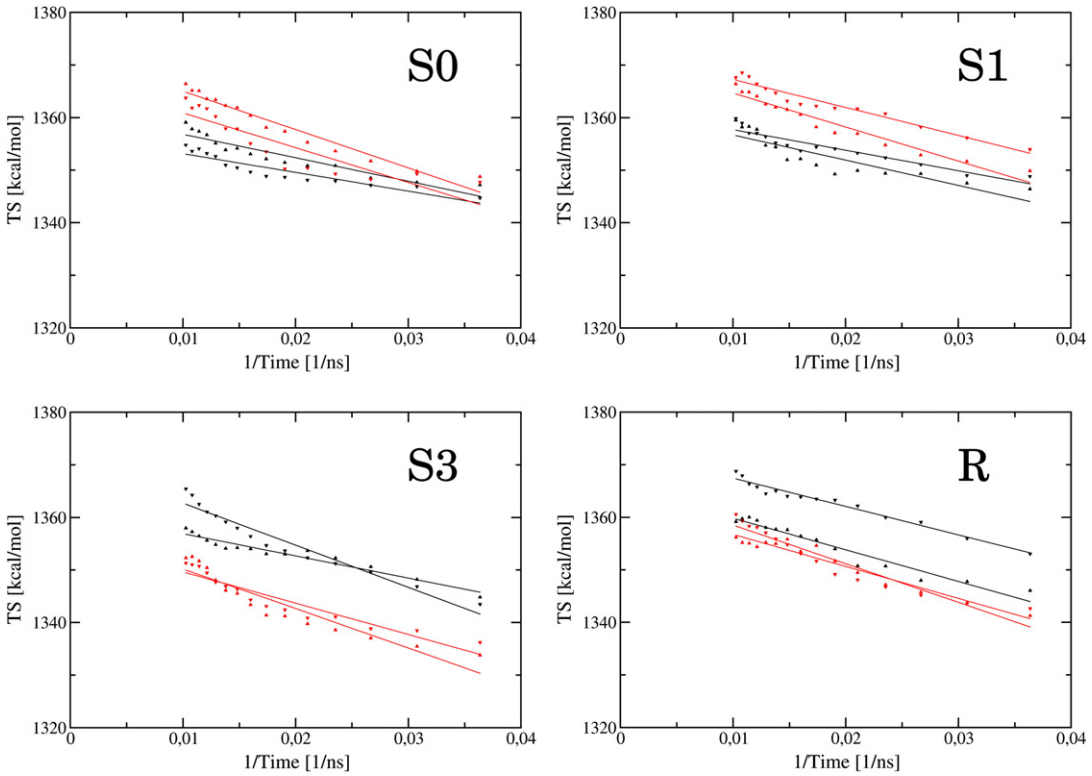

Fig. 3. TS^{TBG} vs equilibrated simulation time^{-1} calculated with Eq. (2) (triangle) and the linear fit to Eq. (3), for last 75 ns of the simulation (solid line); TBG (black) and T4–TBG (red). Both simulation sets 1 (triangle facing up) and 2 (triangle facing down) are shown.

role in determining TBG affinity. As expected, and since similar interactions were observed between the protein and the hormone in all the studied cases, the change in T4 entropy upon binding was very similar for all states (Table 1, column 6). In summary, the analysis of all thermodynamic contributions to the binding free energy shows that only the conformational entropy presents significant changes among the studied TBG states. These changes are consistent with the experimentally observed trend, which shows that increased loop insertion results in lower affinity. According to our data, this is due to a shift from a positive to a negative contribution of the change in the TBG conformational entropy upon binding. In other words, in the high affinity S0 state, conformational entropy increases due to hormone binding, thus contributing favorably to the binding free energy, while in the S3 and R states hormone binding reduces the conformational entropy and this "entropy cost" is translated into a lower affinity.

Given that conformational entropy seems to be responsible for the change in TBG affinity for T4, we looked for the origin of this effect at the dynamics level. Particular attention was given to the lowest frequency modes because they make the largest contribution to the configurational entropy, and are associated with the largest amplitude motions. We, then, analyzed the contribution of each EM to the $T\Delta S_{\infty}^{TBG}$, by computing the difference between the entropy for nth-EM of the free and T4 bound TBG for the simulation set 1. The entropy contribution of each EM was computed using Eq. (6).

$$T\Delta S^{n} = TS^{n}_{T4-TBG} - TS^{n}_{TBG} \quad (6)$$

The values where multiplied by 300 K to obtain $T\Delta S_{\infty}^{nth\text{-}EM}$ in kcal/mol. The resulting $T\Delta S_{\infty}^{nth\text{-}EM}$ vs nth plot for all states is shown in Fig. 4. The results show that there is no general trend, but specific modes contribute differentially to the binding entropy in each case. For example, in the S0 state, EM 2, 3 and 4, significantly diminished their contribution to the entropy upon binding. Comparison of the first four modes between the bound and unbound S0 states, using the SI,

Table 1
Thermodynamic parameters calculated from the MD simulations for thyroxine binding to TBG in different RCL conformations. The energetic values are in kcal/mol ± standard deviation.[a]

System	ΔE_{VdW}	ΔE_{elec}	ΔG^{solv}	$T\Delta S_{\infty}^{TBG}$	$T\Delta S_{\infty}{}^{T4}$	ΔG_B
S0	−47 ± 3	−56 ± 11	62 ± 10	11 ± 5	−30 ± 1	−22
S1	−46 ± 3	−56 ± 12	63 ± 11	10.4 ± 0.8	−31 ± 1	−18
S3	−46 ± 4	−63 ± 15	66 ± 13	−9 ± 6	−32 ± 1	−2
R	−47 ± 3	−58 ± 11	64 ± 10	−5 ± 5	−30 ± 1	−6

[a] $T = 300$ K. ΔE_{VdW} and ΔE_{elec} correspond to the difference in the Van der Waals and electrostatic energy; ΔG^{solv} is the difference in solvation free energy; $T\Delta S_{\infty}^{TBG}$ and $T\Delta S_{\infty}{}^{T4}$ are the TBG and T4 differences in the configurational entropy, respectively. ΔG_B was computed from the other mentioned parameters using Eq. (5). For detailed description of how each parameter was calculated see Methods.

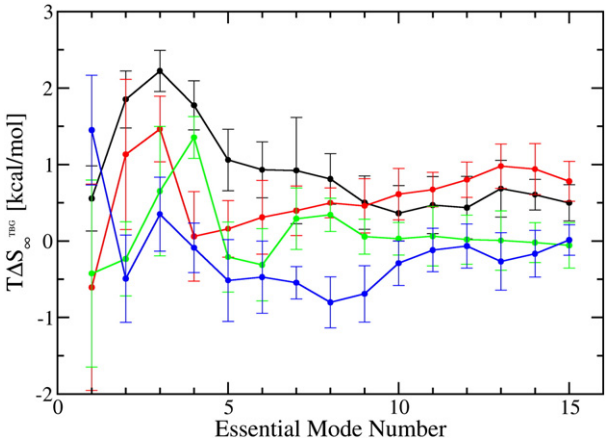

Fig. 4. Entropic contribution of the first 15 essential modes to TBG affinity for T4 in the S0 (black), S1 (red), S3 (green) and R (blue) states computed from the simulation set 1, as compared by Eq. (6).

showed that the modes change significantly between both states with very small overlap (Table S3-S0). This fact points to a significant change in the TBG dynamics upon binding in the S0 state. In the S1 state, the effect is similar with EM 2 and 3 yielding a significant increase in the entropy upon binding. The comparison of modes showed several modes with significant overlap, but not in the same order (Table S3-S1). Interestingly, for these two states almost all $T\Delta S_{\infty}^{nth\text{-}EM}$ values are above zero. In the S3 state, the EM show no general trend, with alternating positive and negative contributions. The mode comparison showed that only some modes displayed minor overlap (Table S3-S3). Finally, for the R state all the first 10 EM, excluding the mode one, showed negative $T\Delta S$ values. There were also several modes showing minor overlap between the S3 and R states.

Given that the second EM follow a positive $T\Delta S_{\infty}^{TBG}$ value in the S0 and S1 sates, while negative in the S3 and R states, we decided to look in detail at the changes of these EM upon T4 binding for each system. The plot of EM displacements vs residue represents the magnitude of each residue movement along the mode. In Fig. S5, the plots for the TBG and T4–TBG systems in the different states are shown. At a glance, no clear general trend is observed, highlighting that a complex change in the dynamics occurs after T4 binding, consistent with the previous similarity index calculation. However, there are several regions that change their mobility pattern, while others remain fairly rigid. The changing regions are parts of hD (residues 81 to 101), hE (residues 124 to 134), hF, (residues 146 to 162), s1C and s2C (residues 200 to 224), the sB4–hG loop (residues 252 to 259), s6A (residues 288 to 295), and hI (residues 297 to 304). Interestingly, this dynamically changing regions overlap with recent Hydrogen/Deuterium Exchange Mass Spectrometry experiments, studying the native state dynamics of the human serpin αAT. Those experiments showed that the residues located in hA, hD, hE, hF, hH, s6A and s1C secondary structure elements were those which contributed most to protein dynamics [35]. In all systems, however, there is a clear change in the EM displacement pattern upon binding (red and black plots). In addition, the 2nd EM of the R, and to a lesser extent, of the S3 sate, are much more localized in specific protein regions than that of the S0 and S1 states, especially in the unbound state. This is evidenced as sharp and stronger peaks in Fig. S5. Thus, again, analysis of one representative mode highlights that changes in protein dynamics that determine the differential entropy contribution are global and cannot be localized or assigned to a particular structural feature.

In summary, these results strongly suggest that the change in protein dynamics that modulates the ligand affinity is related to global, non-specific, low frequency motions of the protein. These strongly depend on the RCL insertion degree.

4. Discussion

A common feature of several biochemical processes is that they occur in conjunction with significant structural change of the involved protein. Thus, allosteric effects are commonly explained solely in terms of the structural changes associated with process as those observed for the hormone binding to the TBG and CBG serpins. Then based on the T4–TBG crystal structure it was suggested that the incorporation of Thr342 as an incipient s4A strand will induce a reorientation of the Tyr241 side chain (located in the β-sheet B) followed by a distortion of T4 binding site. The final result is a less favorable architecture for thyroxine binding and the consequent drop in affinity [8]. However, when chimeric αAT–T4–cTBG and αAT–cTBG crystals were solved, it was observed that Tyr241 side chain remained in the same conformation than in the non-cleaved RCL structure, and with the same hydrogen bond interactions [10], casting serious doubts on the above described structural interpretation of TBG allosteric regulation of T4 affinity (see Fig. 5 of ref. [10]). In agreement with these results, reorientations or structural changes affecting the Tyr241 side chain upon Thr342 incorporation were not detected during our extensive simulations in the systems of free and complexed TBG, in both S3 and R states. Moreover, neither significant structural changes, nor changes in the T4–TBG interactions were observed among the four simulated states. Therefore, the subtle allosteric modulation of the affinity mediated by RCL insertion is not governed by TBG structural changes in the binding site, but by changes in its dynamics and entropy contributions to T4 binding.

Entropy or dynamically governed allosteric processes have been previously reported. For example, in glycopeptide antibiotics such as vancomycin, the positive cooperativity effects are not accompanied by significant structural changes at the monomer level and calorimetric studies show no change in the enthalpy contribution to the second ligand binding, suggesting that the free energy gain of the second ligand (i.e. the cooperativity effect) is entropy driven. To understand the molecular basis of this cooperative effect, the authors performed MD simulations of vancomycin in the absence and presence of the ligand, in the monomeric and dimeric states. Both processes, dimerization and ligand binding, were found to shift the internal vibrational modes of vancomycin to higher frequencies with less amplitude, thus reducing the entropy. Interestingly, the first process always reduces the entropy more than the second, leading to the observed cooperativity [14]. Quantitative analysis of the entropy change upon ligand binding and dimerization using the EM consistently shows that positive cooperativity is entropy driven, verifying the Cooper–Dryden model. Briefly, the model postulates that ligand-induced (or dimerization) changes in protein dynamics could produce allosteric communication between distinct binding sites, even in the absence of evident macromolecular conformational changes. The effect would be evidenced by changes in the frequencies and amplitudes of the macromolecular thermal fluctuation in response to the process [36,37]. The results here presented are also in agreement with the Cooper–Dryden model, since a clear change in the low frequencies EM of TBG upon T4 binding is observed in relation to the RCL insertion degree. This results in an entropically driven allosteric modulation of T4 binding due to RCL state.

Experimentally, the RCL cleavage in TBG results in a 3-times decrease in the binding (or affinity) constant. Since, the particular structure of the S state is not well defined, and several S states have been suggested to exist in equilibrium with different degrees of loop insertion, it is difficult to compare these results directly with our data. Moreover, although the hallmark of the allosteric transition in serpins is related to the S to R transformation, upon RCL cleavage, experimental studies on chimeric proteins with different RCL lengths have shown that different subpopulations of the S state may exist, displaying different affinities for the hormone. Different RCL chimeric proteins, with varying loop lengths and insertion grades, have shown that longer loops (i.e. with higher degree of insertion) displayed lower affinities [12,13]. Our results from the different S states, are in agreement with the general idea that subpopulations of the S state exist, and that they exhibit different affinities for the hormone. In particular, significant differences were observed between the affinity of the S0/S1 states and the S3/R states. From a structural point of view, it should be noted that the main difference between the S3 and the other S states is associated to the incorporation of the Thr342 into the TBG core as part of s4A, suggesting that this event has a key role in the process. This fact is consistent with mutagenesis experimental data for TBG and CBG (where the equivalent residue corresponds to Thr388) that showed the key role of this residue in relation to RCL incorporation as s4A in the R state [10,13]. On the other hand, since no significant changes are observed between the S3 and R states, the existence of a limit in the effect of RCL insertion is derived. Indeed, experimental data suggested that there is a limit in the binding affinity effect, since chimeric TBG proteins with long RCL showed similar affinity whether or not the loop was cleavage [12]. Finally, the RCL cleavage has been linked in many serpins with a change in thermal stability, evidencing the importance of the entropic contributions, as observed here.

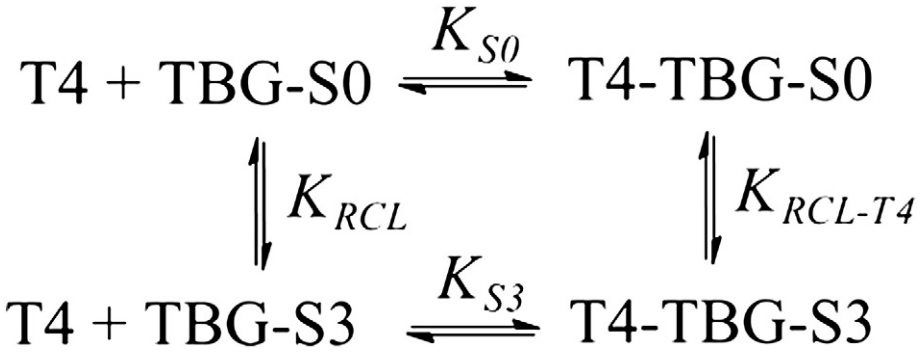

Scheme 1. Thermodynamic scheme relating binding and RCL insertion between the S0 and S3 states. K_{S0} and K_{S3} are the affinity constants of TBG in the S0 and S3 states, respectively; and K_{RCL} and $K_{RCL\text{-}T4}$ are the RCL insertion equilibrium constants in the free and T4-bound proteins.

From a biological point of view, the role of the increased thyroxine release from TBG after the S-to-R transition is not clear. In addition, the biological role of the potentially different accessible S states, which also show different binding affinities is completely unknown. In this context, the analysis of the S0-to-S3-to-R allosteric transition was based on the relation between TBG states and T4 affinities from a pure thermodynamic viewpoint. For simplicity, we consider only the S0 and S3 states, corresponding to a high and low T4 affinity, respectively. K_{S0} and K_{S3} were the related equilibrium constants. K_{RCL} characterizes the RCL insertion in the transition from S0 to S3 in the absence of T4, and $K_{RCL\text{-}T4}$ is the constant for RCL insertion in the presence of the bounded hormone. The four constants and the corresponding states are related according to Scheme 1.

According to Scheme 1, the relation between the free energies for each process can be expressed by Eq. (7),

$$\Delta G_{S0} + \Delta G_{RCL-T4} = \Delta G_{RCL} + \Delta G_{S3} \tag{7}$$

and the relationship among the corresponding equilibrium constants is

$$\frac{K_{S0}}{K_{S3}} = \frac{K_{RCL}}{K_{RCL-T4}}. \tag{8}$$

Eqs. (7) and (8) are well known to describe allosteric systems where a conformational change (e.g. the degree of RCL insertion as s4A) is related to a given ligand affinity (here, the T4 hormone).

Implications of the presented analysis in the context of our results for TBG are discussed. According to both, those experimental and our results, the binding equilibrium constants are such $K_{S0} > K_{S3}$. Eq. (8) indicates that $K_{RCL} > K_{RCL\text{-}T4}$, which means that the equilibrium is shifted towards the RCL inserted state in the absence of the hormone, when compared to the same equilibrium in its presence. On the other hand, the equilibrium constant that characterizes RCL insertion is smaller when the hormone is bound to the protein than when it is absent, and thus the equilibrium is shifted to the conformations with increased loop exposure. If this relationship between the affinity and the degree of RCL insertion is maintained for different S states, the same analysis and conclusion apply, meaning that T4 binding drives TBG to a more exposed RCL conformations, and vice-versa. In the physiological context it could be possible that while in the free protein population the loop is “hidden” inside the protein body, in the hormone bound TBG population a more exposed RCL is present, which makes it more accessible to the action of proteases. In other words, proteases will preferentially target those TBG proteins carrying T4, promoting the release after S-to-R transition and final drop in affinity. This discussion can also be applied to CBG protein and other serpin. Thus, the existence of multiple S states with different affinities and RCL exposure may allow a more efficient (or faster) site specific hormone release (T4 from TBG and corticosteroid from CBG) due to the action of tissue specific proteases. How this allosteric effect, that promotes and accelerates hormone release upon cleavage, is exploited by tissue factors, that specifically target and cut TBG (or CBG) under certain circumstances, is an open and emerging issue related to T4 physiological role.

5. Conclusion

To understand the allosteric modulation of thyroxine affinity by the degree of RCL incorporation as an s4A strand in TBG [12,13,38], we performed MD simulation of TBG in three different S states and the R state, in the presence and absence of thyroxine bound. Our results showed that the hormone performs similar interactions with the TBG protein in all states, in good agreement with crystallographic data [8,10]. Decomposition of the binding free energy into enthalpic, entropic and solvent contributions showed that no significant difference was observed considering solely the enthalpic and solvent contributions. However, a clear decrease in the protein configurational entropy upon thyroxine binding was observed when the RCL was incorporated as s4A strand. This results in a decrease of the binding free energy when transition goes from the S0 to the S3 and/or R state. Moreover, small differences in binding affinity are observed between S0 and S1 states as well as between S3 and R states, highlighting the relevance of the Thr342 residue inserted as an s4A. Our results support the idea that Thr342 insertion in to the TBG core triggers the decrease in the T4 affinity, while successive incorporation of residues as s4A does not affect significantly the T4 binding. A fact that is consistent with available experimental data of chimeric TBG proteins with RCL of different lengths. Finally, we analyzed the possible role of the presence of multiple S states with different T4 affinities and proposed a possible physiological role for the observed effects. In summary, TBG presents another example of an entropy driven allosteric protein.

Acknowledgements

AAP is grateful to CONICET for a Doctoral Fellowship. RMSA and MAM are members of CONICET. The discussions with Ramiro G. Rodríguez Limardo and Carlos M. A. Guardia about entropy were useful to this work. Computer power was gently provided by CeCAR at FCEN-UBA and SimOne at INSIBIO-CONICET. This work was partially supported by grants from Universidad Nacional de Tucumán (CIUNT 26/D405) and CONICET (PIP 0303).

Appendix A. Supplementary data

Supplementary data to this article can be found online at http://dx.doi.org/10.1016/j.bbagen.2013.02.023.

References

[1] A.J. Hulbert, Thyroid hormones and their effects: a new perspective, Biol. Rev. 75 (2000) 519–631.
[2] J.A. Irving, R.N. Pike, A.M. Lesk, J.C. Whisstock, Phylogeny of the serpin superfamily: implications of patterns of amino acid conservation for structure and function, Genome Res. 10 (2000) 1845–1864.
[3] P.G.W. Gettins, Serpin structure, mechanism, and function, Chem. Rev. 102 (2002) 4751–4804.
[4] P.A. Pemberton, P.E. Stein, M.B. Pepys, J.M. Potter, R.W. Carrell, Hormone binding globulins undergo serpin conformational change in inflammation, Nature 336 (1988) 257–258.
[5] O.E. Janssen, H.M.B. Golcher, H. Grasberger, B. Saller, K. Mann, S. Refetoff, Characterization of T4-binding globulin cleaved by human leukocyte elastase, J. Clin. Endocrinol. Metab. 87 (2002) 1217–1222.
[6] B. Jirasakuldech, G.C. Schussler, M.G. Yap, H. Drew, A. Josephson, J. Michl, A characteristic serpin cleavage product of thyroxine-binding globulin appears in sepsis sera, J. Clin. Endocrinol. Metab. 85 (2000) 3996–3999.
[7] M.A. Klieber, C. Underhill, G.L. Hammond, Y.A. Muller, Corticosteroid-binding globulin, a structural basis for steroid transport and proteinase-triggered release, J. Biol. Chem. 282 (2007) 29594–29603.
[8] A. Zhou, Z. Wei, R.J. Read, R.W. Carrell, Structural mechanism for the carriage and release of thyroxine in the blood, PNAS 103 (2006) 13321–13326.
[9] A.J. McCoy, X.Y. Pei, R. Skinner, J.-P. Abrahams, R.W. Carrell, Structure of beta-antithrombin and the effect of glycosylation on antithrombin's heparin affinity and activity, J. Mol. Biol. 326 (2003) 823–833.
[10] X. Qi, F. Loiseau, W.L. Chan, Y. Yan, Z. Wei, L.-G. Milroy, R.M. Myers, S.V. Ley, R.J. Read, R.W. Carrell, A. Zhou, Allosteric modulation of hormone release from thyroxine and corticosteroid-binding globulins, J. Biol. Chem. 286 (2011) 16163–16173.
[11] A. Zhou, Z. Wei, P.L.D. Stanley, R.J. Read, P.E. Stein, R.W. Carrell, The S-to-R transition of corticosteroid-binding globulin and the mechanism of hormone release, J. Mol. Biol. 380 (2008) 244–251.
[12] H. Grasberger, H.M.B. Golcher, A. Fingerhut, O.E. Janssen, Loop variants of the serpin thyroxine-binding globulin: implications for hormone release upon limited proteolysis, Biochem. J. 365 (2002) 311–316.
[13] H.-Y. Lin, C. Underhill, B.R. Gardill, Y.A. Muller, G.L. Hammond, Residues in the human corticosteroid-binding globulin reactive center loop that influence steroid binding before and after elastase cleavage, J. Biol. Chem. 284 (2009) 884–896.
[14] S. Jusuf, P.J. Loll, P.H. Axelsen, Configurational entropy and cooperativity between ligand binding and dimerization in glycopeptide antibiotics, J. Am. Chem. Soc. 125 (2003) 3988–3994.
[15] D.F. Gauto, C. Modenutti, V.G. Dumas, L. Alvarez, J.P. Bustamante, A.G. Turjanski, M.A. Marti, Determining free energy of protein–ligand binding and association/dissociation processes using computer simulations, World Res. J. Pept. Protein 1 (2012) 21–32.
[16] A. Sali, MODELLER 9.9, University of California San Francisco, San Francisco, USA, 2009.
[17] H.J.C. Berendsen, J.P.M. Postma, W.F. van Gunsteren, A. DiNola, J.R. Haak, Molecular dynamics with coupling to an external bath, J. Chem. Phys. 81 (1984) 3684–3690.
[18] J.-P. Ryckaert, G. Ciccotti, H.J.C. Berendsen, Numerical integration of the Cartesian equations of motion of a system with constraints: molecular dynamics of n-alkanes, J. Comp. Physiol. 23 (1977) 327–341.
[19] V. Daggett, Protein simulations, 1.a ed., Advances in Protein Chemistry, vol. 66, Academic Press, 2003.
[20] J. Wang, R.M. Wolf, J.W. Caldwell, P.A. Kollman, D.A. Case, Development and testing of a general amber force field, J. Comp. Chem. 25 (2004) 1157–1174.
[21] A.A. Petruk, M.A. Marti, R.M.S. Alvarez, Thyroid hormone interactions with DMPC bilayers. A molecular dynamics study, J. Phys. Chem. B 113 (2009) 13357–13364.
[22] D.A. Case, T.A. Darden, T.E. Cheatham III, C.L. Simmerling, J. Wang, R.E. Duke, R. Luo, R.C. Walker, W. Zhang, K.M. Merz, B. Roberts, B. Wang, S. Hayik, A. Roitberg, G. Seabra, I. Kolossvai, K.F. Wong, F. Paesani, J. Vanicek, J. Liu, X. Wu, S.R. Brozell, T. Steinbrecher, H. Gohlke, Q. Cai, X. Ye, J. Wang, M.-J. Hiseh, G. Cui, D.R. Roe, D.H. Mathews, M.G. Seetin, C. Sagui, V. Babin, T. Abe, S. Gusarov, A. Kovalenko, P.A. Kollman, AMBER 11, University of California, San Francisco, 2010.
[23] W. Humphrey, A. Dalke, K. Schulten, VMD: visual molecular dynamics, J. Mol. Graph. 14 (1996) 33–38.
[24] W.C. Still, A. Tempczyk, R.C. Hawley, T. Hendrickson, Semianalytical treatment of solvation for molecular mechanics and dynamics, J. Am. Chem. Soc. 112 (1990) 6127–6129.
[25] B.N. Dominy, C.L. Brooks, Development of a generalized Born model parametrization for proteins and nucleic acids, J. Phys. Chem. B 103 (1999) 3765–3773.
[26] D.F. Gauto, S. Di Lella, D.A. Estrin, H.L. Monaco, M.A. Martí, Structural basis for ligand recognition in a mushroom lectin: solvent structure as specificity predictor, Carbohydr. Res. 346 (2011) 939–948.
[27] C.M.A. Guardia, D.F. Gauto, S. Di Lella, G.A. Rabinovich, M.A. Martí, D.A. Estrin, An integrated computational analysis of the structure, dynamics, and ligand binding interactions of the human galectin network, J. Chem. Inf. Model. 51 (2011) 1918–1930.
[28] I. Massova, P. Kollman, Combined molecular mechanical and continuum solvent approach (MM-PBSA/GBSA) to predict ligand binding, Perspect. Drug Discov. Des. 18 (2000) 113–135.
[29] I. Andricioaei, M. Karplus, On the calculation of entropy from covariance matrices of the atomic fluctuations, J. Chem. Phys. 115 (2001) 6289–6292.
[30] S. Di Lella, M.A. Martí, D.O. Croci, C.M.A. Guardia, J.C. Díaz-Ricci, G.A. Rabinovich, J.J. Caramelo, D.A. Estrin, Linking the structure and thermal stability of β-galactoside-binding protein galectin-1 to ligand binding and dimerization equilibria, Biochemistry 49 (2010) 7652–7658.
[31] J. Dolenc, S. Gerster, W.F. van Gunsteren, Molecular dynamics simulations shed light on the enthalpic and entropic driving forces that govern the sequence specific recognition between netropsin and DNA, J. Phys. Chem. B 114 (2010) 11164–11172.
[32] M. Kolář, T. Kubař, P. Hobza, Sequence-dependent configurational entropy change of DNA upon intercalation, J. Phys. Chem. B 114 (2010) 13446–13454.
[33] P. Arroyo Mañez, C. Lu, L. Boechi, M.A. Marti, M. Shepherd, J.L. Wilson, R.K. Poole, F.J. Luque, S.-R. Yeh, D.A. Estrin, Role of the distal hydrogen-bonding network in regulating oxygen affinity in the truncated hemoglobin III from *Campylobacter jejuni*, Biochemistry 50 (2011) 3946–3956.
[34] L. Capece, D.A. Estrin, M.A. Marti, Dynamical characterization of the heme NO oxygen binding (HNOX) domain. Insight into soluble guanylate cyclase allosteric transition†, Biochemistry 47 (2008) 9416–9427.
[35] Y. Tsutsui, L. Liu, A. Gershenson, P.L. Wintrode, The conformational dynamics of a metastable serpin studied by hydrogen exchange and mass spectrometry, Biochemistry 45 (2006) 6561–6569.
[36] A. Cooper, D.T.F. Dryden, Allostery without conformational change, Eur. Biophys. J. 11 (1984) 103–109.
[37] D. Kern, E.R. Zuiderweg, The role of dynamics in allosteric regulation, Curr. Opin. Struct. Biol. 13 (2003) 748–757.
[38] H.-Y. Lin, Y.A. Muller, G.L. Hammond, Molecular and structural basis of steroid hormone binding and release from corticosteroid-binding globulin, Mol. Cell. Endocrinol. 316 (2010) 3–12.